Tools for conductance measurements of metallic and molecular nanowires

Thomas Leoni, Monzer Alwan, Hubert Klein, Nadine Candoni, Aude Lereu, Philippe Dumas

Tools for conductance measurements of metallic and molecular nanowires

Thomas Leoni, Monzer Alwan, Hubert Klein, Nadine Candoni, Aude L. Lereu, Philippe Dumas*

CINaM CNRS, UPR 3118 & Aix-Marseille Université Faculté des Sciences de Luminy, 13288 Marseille Cedex 9, France

**Author for correspondence: Philippe Dumas, email: dumas@cinam.univ-mrs.fr*

Abstract

Conductance-elongation curves of gold nanojunctions exhibit characteristic plateaus just prior to breaking. Conductances of these plateaus are integer multiples of the quantum of conductance. These plateaus occur because, in this size regime, transport is ballistic and the conductance is independent of the length of the nanojunction. We developed a STM-based break junction technique to access to the conductance-elongation curves. In this paper, specific tools adapted for measurements in solution are described. We then report on our results obtained for both metallic and molecular nanowires.

Keywords: Single molecule conductance; Break junction; Ballistic transport

1. Introduction

During the last decades, the study of conductance in metallic nanowires has interested many groups employing different techniques to investigate electron transport which is ballistic at the nanometer scale.

One of the first techniques, to access to these conductance measurements in atomic-sized contacts, employs Scanning Tunneling Microscopy in Break Junction regime (referred to as STM-BJ) [1,2]. In STM-BJ, one measures the conductance between a tunnel tip and a metallic surface. In the case of a gold tip and a gold surface, the current between the contact point and the vacuum tunneling, displays a transition stage. This transition occurs in the nanoscale working regime meaning that the junction length becomes smaller than the electron elastic mean free path. Hence, the conductance is expected to become invariant with the junction length. This regime is referred to the ballistic regime. The transition, between contact and tunneling regime, explores the ballistic regime and conductance-elongation curves exhibit characteristic plateaus. These plateaus are multiples of the Landauer quantum of conductance $G_0=2e^2/h$, where h is Planck's constant and e the electron charge [3]. Recently, we have experimentally and numerically studied the configuration of gold nanowires at these plateaus [4, 5]. We have correlated the appearance of the plateaus at G_0 for monoatomic nanowires and $2G_0$ for diatomic nanowires linking the tunneling tip to the surface.

STM-BJ is a very robust technique that has been used in a broad range of experimental conditions, ranging from cryogenic temperatures to ambient or from ultra-high vacuum to atmospheric pressure or even in liquids [6]. In reference 6, the authors demonstrate the use of STM-BJ for conductance measurements of molecules. They utilize liquids made of "insulating" solvents containing a small amount of "conducting" molecules. These latter possess specific atoms allowing them to attach to the gold electrodes. In this case, one molecule can bridge the gap of the nanojunction modifying the conductance. The resulting conductance-elongation curves evidence then the presence of this molecule and give the conductance value in a straightforward way [6].

In this paper, we present the investigation of single molecule conductance measurements by STM-BJ. We first describe the appropriate tools developments for molecular measurements. These tools include the experimental setup as well as software developments to extract information from the raw experimental data. Although we do not describe the software itself, the main choices for the algorithms are exposed. Thereafter, we discuss the results obtained with gold nanowires and with bipyridine molecules. A comparison with the recent work reported in [7,8], is then presented. Finally, we conclude on the ability of STM-BJ to gain information in term of contact

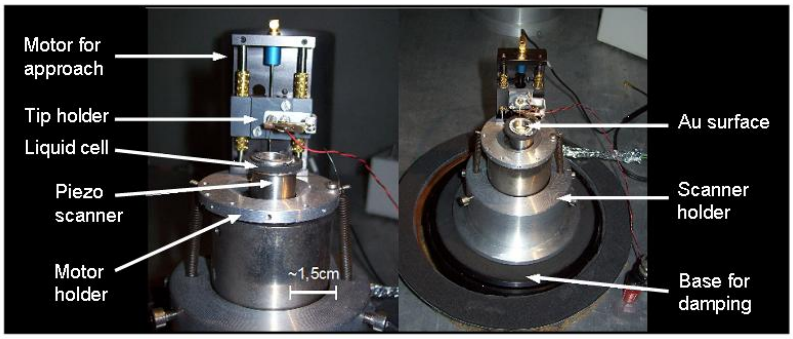

Figure 1. STM-BJ setup. The tip, mounted on the approach motor, is immersed into the all stainless steel liquid cell down to the gold surface (see Figure 2a). The liquid cell is supported by the xyz-piezo scanner. The whole system is isolated from mechanical vibrations and shielded by a Faraday cage.

geometry and in term of electronic transport through single molecules.

2. Experimental

In our experiment, we developed a home-made Scanning Tunneling Microscope (STM) (see Figure 1). The specific hardware is driven by dedicated software so the STM operates as a break junction. Hereafter, the resulting instrument will be referred to as STM-BJ.

This STM-BJ was used to investigate the conductance of gold atomic nanowires and of 4-4' bipyridine (thereafter named bipy and depicted in Figure 2b). To immerse the gold surface and tip into the bipy solution, a stainless steel liquid cell (volume ~ 0,3 mL) is designed and placed on the top of the STM z-piezo as depicted in Figure 1. At the bottom of the liquid cell, the studied surface is positioned. This latter is a 100 nm gold surface evaporated on a freshly cleaved mica substrate. Details of this preparation can be found elsewhere [9]. The liquid cell is then filled with a millimolar solution of 4-4' bipyridine in toluene covering the surface. Thereafter, a gold tip (Goodfellow, purity 99.99+%) is immersed in the solution using a step by step translation stage (MS30, Mechonics) as depicted in Figure 2a). This mechanical part as well as the I/V converter (described below) are placed inside a Faraday cage to minimize external electrical disturbances.

Since we aim in measuring both bipy current (typically hundreds of picoampers) and gold nanowire current (typically ten microampers) a high dynamical range of currents is required. We thus developed a quasi-logarithmic I/V converter based on the work reported in reference [10]. The principle is the voltage drop of a diode that is a logarithm function of the current across the diode

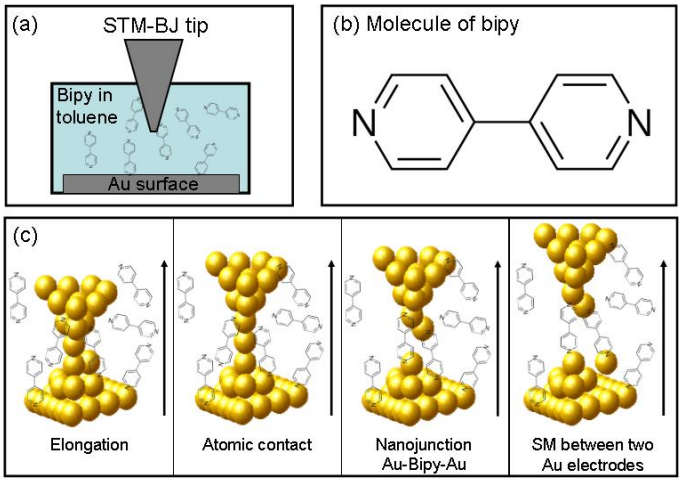

Figure 2. (a) Scheme of the STM-BJ in solution. In this study the solution is a millimolar solution of 4-4' bipyridine (bipy) in toluene. (b) Representation of a bipy molecule. (c) Schematics of the pulling process in solution from the gold atomic contact until the single molecule (SM) contact.

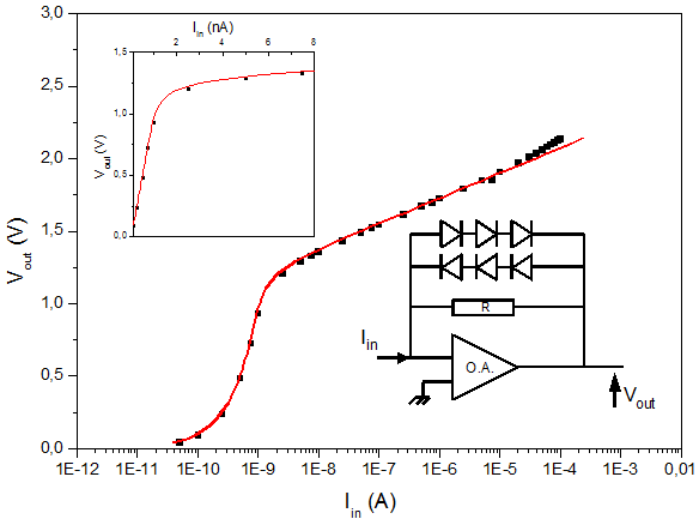

Figure 3. Calibration curve of the logarithmic amplifier. The dotted curve corresponds to measurements and the continuous (red) curve corresponds to the analytical fit. The logarithmic behavior above 2.10^{-9}A is due to the diodes whereas the linear behavior in the low current regime (see upper inset) results from the feedback resistor. The lower inset gives a scheme of the I/V converter.

(sensitivity approx. 50mV/current decade/diode). A schematic diagram is shown in the lower inset of Figure 3. Indeed, by cascading several diodes in series, we know that the sensitivity will proportionally increase. Furthermore, mounting two resulting dipoles in parallel, in opposite direction, will allow the current to flow in both directions. In our case, we utilize two dipoles in parallel consisting by three diodes in series. We also add a high impedance resistor in a third branch in parallel to the dipoles in order to improve the sensitivity in the low current regime (see upper inset of Figure 3). This association of diodes and resistor is then used to feedback a low input bias current op-amp (OPA111, Burr Brown) allowing to bias the tip at the virtual ground while the surface is polarized. This device permits to measure at least currents ranging over 7 orders of magnitude (see Figure 3). With the typical values (10-100 mV) used to bias the nanojunction, one measures conductances between $10^{-5}G_0$ and $10^{2}G_0$ (i.e. from tunneling regime to short circuit). This home-made I/V converter is then carefully calibrated under experimental conditions. Finally, the voltage output of the I/V converter is read by an input/output card (National Instrument 6259) that is also used to control the z-piezo (Z sensitivity ~ 2 nm/V) and the approach stepper motor of the STM-BJ. Beside, the acquisition card is piloted by a dedicated program, encoded in Labview, to ensure constant current by feedbacking the z-position. The feedback loop can also be temporally disabled to indent deliberately the surface with the tip. This is the way we create a nanojunction which will be broken (Break Junction or BJ technique) by pulling the surface away from the tip. Figure 2c explains the formation of the nanojunction until breaking into two electrodes. During the pulling, the current is recorded providing a conductance-elongation curve. The feedback loop is then switched back on. The whole sequence can be carried out a large number of times (up to several hundreds of thousands) to provide statistics [4].

Although noteworthy, is that with our STM-BJ, we use typical z-ramp speeds for the approach-pulling cycle of 100 pm/ms (determined by z-piezo calibration). Therefore a cycle lasts approximately 100 ms. At this time scale, undesired drift can be neglected. However, it is also interesting to study the breaking mechanism at much lower pulling speeds but in this case, much more "rigid" devices such as mechanically controlled break junctions (MCBJ) [11,12], are needed.

Finally, acquisition software tools are implemented in order to display, in real time, two important information. The first one is the conductance curves from the measured current. The second one is the conductance histogram corresponding to the conductance occurrence as a function of the conductance. The conductance histogram shows the preferred conductance values and statistically reveals conductance plateaus. More complex analysis, such as automatic detections of the plateaus, length histograms [4], 2D-histograms, correlations between events and so on, are performed off-line.

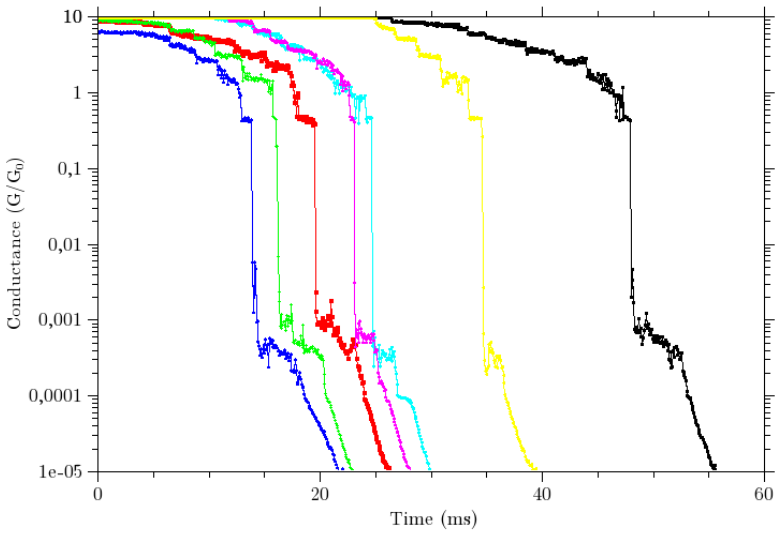

Figure 4. Typical conductance-elongation curves exhibiting plateaus attributed to gold contacts (high conductance regime) and molecular contacts (low conductance regime).

3. Results and Discussion

In this study, we benefit from the conductance measurements to discriminate between gold and molecular nanowires. We choose here bipy (molecule representation Figure 2b) as a model system and because it is a well-known bidentate metal ligand in solution due to the donor pairs of its nitrogen atoms. This characteristic permits the bipy to easily graft onto gold surfaces as evidenced by surface enhanced Raman scattering [13], and STM studies [14].

When pulling until breaking a gold nanojunction immersed in a toluene solution containing bipy molecules, two series of plateaus are observed on the conductance-elongation curves. This is shown in Figure 4. The ballistic transport of electrons (through the nanojunction) explains the existence of these plateaus. Indeed within ballistic transport, the conductance does not depend on the stretching of the nanojunction as long as no changes in waist are induced.

Note that in Figure 4, the horizontal axis is in time units (ms) corresponding to raw data. However, the pulling speed (here 80 pm/ms) in our apparatus is known (through piezo calibration) thus the horizontal axis is directly proportional to the elongation.

The wide dynamic range of the dedicated I/V converter, described in the experiment section, allows the observation of the ballistic transport through gold nanowires and through bipy within the same conductance-elongation curve. In Figure 4, we plot selected measured conductance-elongation curves highlighting characteristic plateaus. Two series of characteristic plateaus are observed, one for $G/G_0 \sim 1$ and one below 10^{-3}.

The plateaus at G_0 and NG_0, where N is an integer, are characteristic of the ballistic transport in gold nanowires with monoatomic and N-atomic waists respectively.

The second set of plateaus at lower values can be attributed to the presence of bipy. Between the gold plateaus and the ones of bipy, we observe a very rapid drop of ~3 orders of magnitude in the conductance. This drop coincides with the breaking of the last monoatomic gold nanowire resulting in two nanometer-separated electrodes (Figure 2c). In fact, just prior to breaking, the gold monoatomic nanowire is under tension [15], after breaking the apex of the two electrodes relax and separate faster than the applied pulling speed [16]. At this stage, bipy molecules from the solution or grafted onto the electrodes can bridge the gap resulting in a metal-molecule-metal nanojunction (see right inset of Figure 2c).

We introduced, in the experiment section, the conductance histogram which is a very common statistical tool used in such studies. As we mentioned earlier, the conductance range is spread out from around G_0 for gold to $10^{-4}G_0$ for bipy. Therefore, in order to clearly display the plateaus for both entities, we plot the conductance histogram in logarithmic scale [17]. Figure 5 shows such a conductance histogram constructed from hundreds of conductance-elongation curves. The peak due to monoatomic gold nanowires is clearly visible at $G/G_0=1$. In addition, below $10^{-3}G_0$, features are

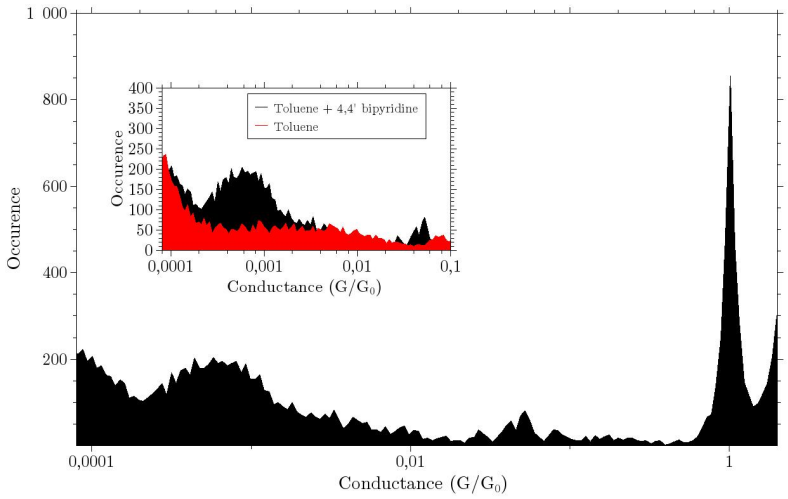

Figure 5. Conductance histogram showing the peak at $G/G_0=1$ and the broader peak due to the contribution of bipy between 10^{-4} and 10^{-3}. The inset displays the additional contribution of bipy (black) with respect to pure toluene (red).

attributed to bipy conductance. The inset of Figure 5 is a zoom in the low-conductance regime together with the pure toluene (the solvent) histogram. The bipy contribution is observed with an average value of $6.10^{-4}G_0$. This is in very good agreement with recent publications from Xiamen University [7], and Columbia University [8], but quite far from the pioneering work of Arizona State University [6]. A potential explanation of this discrepancy is that we construct histograms using every acquired conductance curves. Furthermore, since we work in a wide dynamic range of conductances, we include almost every possible atomic configurations of the molecule. This also demonstrates the importance of carrying out statistical studies.

We now intend to go one step beyond in the discussion. When looking into more details in the data plotted in Figure 4, we can see that all the behaviors of the bipy plateaus are similar from one curve to another. We evidence this observation, by superimposing the conductance-elongation curves in a way that the rapid drops after G_0 coincide. Instead of computing the classical conductance-histogram (as in Figure 5) we compute a conductance-elongation histogram as also used in [8]. This 2D histogram is shown in Figure 6. The bipy contribution, between $2.10^{-4}G_0$ to $2.10^{-3}G_0$, is now displayed more

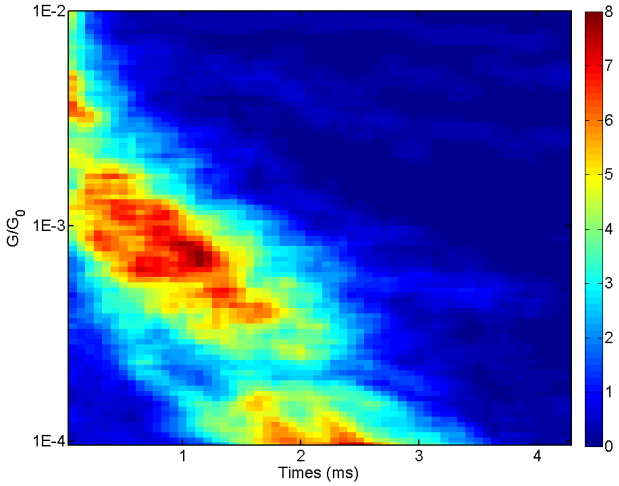

Figure 6. Conductance-elongation histogram proving the effect of the electrodes separation on the bipy conductance. The color scale gives the probability to measure a given molecular conductance for a given metallic electrodes separation.

precisely. By doing so, we prove that the separation distance between the two metallic electrodes influences the conductance through bipy. Figure 6 shows an exponential decay of the conductance with elongation. Possible explanations such as the variation of the angle between the nitrogen-gold bond and the bipy conducting π -system have already been proposed [8]. However, a large number of atomic scenarios can lead to exponential decays. For instance, the progressive decrease (when pulling) of the overlapping between the orbitals of one electrode and the π –system of the molecules can also lead to an exponential behavior. Therefore, one still needs more experimental studies, statistics and comparisons with calculations to be able to sort the potential mechanisms.

Finally, despite lots of improvements, the electrical conductance of single molecules still deserves attention. It has been shown that, even for model molecules such as alkyldithiols, a very large dispersion of the results is observed [18]. This dispersion is first of all due to the large panel of techniques used. Secondly, some techniques extrapolate the single molecule conductance from measurements carried out on a very large number of molecules self-assembled in parallel. In these "averaging" techniques, we cannot rule out important contribution coming from unavoidable defects. Although there is still a long way to fully understand measurements carried out by STM-BJ, this technique has shown its potential in reducing the dispersion for single molecule conductance measurements. We are convinced that STM-BJ will contribute to a better understanding of molecular electronic transport. One of the reasons comes from measurements of single nanojunctions sequentially. *A posteriori*, statistics is then achievable without loosing the advantage to look individually at single events and may be to sort them by configurations.

4. Conclusions

In conclusion, we have shown ballistic transport measurements of metallic and molecular nanowires. We have insisted on the importance in analyzing data taking into account every conductance curves. This is a requirement when questing for unknown molecular conductance plateaus. To achieve this goal, we utilized a specific acquisition (and analysis) with the appropriate dynamic range. The asset is the logarithmic current-voltage converter for acquisition together with its analysis' counterpart that is the logarithm histogram. We evidenced the average contribution of bipy molecules at $6.10^{-4}G_0$ in agreement with recent measurements [7,8]. A deeper analysis using a 2D histogram gives further insights in the atomic evolution of the pulled nanojunction. We thus proved that the separation distance between electrodes contribute to the control of single molecule conductance. We believe that STM-BJ and MCBJ techniques, based on single nanojunction measurements and thereafter statistics, provide unique opportunities to understand the intimacy of molecule/electrode contacts at the atomic scale. Mastering these contacts is of prior importance for the development of potential single molecule electronics applications.

Acknowledgements

The authors would like to acknowledge Nicolas Battaglini and Sabrina Homri for their interest in the instrumental development.

References

1. Agraït, N., Yeyati, A. L., & Ruitenbeek, J. M. V., entPhys. Rep. 377 (2003) 81.
2. Agrait N., Rodrigo J. G., & Vieira S., Phys. Rev. B. 47 (1993) 12345.
3. Landauer, R., IBM J. Res. Dev. 1 (1957) 223.
4. Leoni, T., Zoubkoff, R., Homri, S., Candoni, N., Vidakovic, P., Ranguis, A., Klein, H., et al., Nanotechnology 19 (2008) 355401.
5. Klein, H., et al., An atomistic picture of conductance bistabilities in gold point contacts at 100K (To be submitted).
6. Xu, B., & Tao, N. J., Science 301 (2003) 1221.
7. Zhou, X., Chen, Z., Liu, S., Jin, S., Liu, L., Zhang, H., Xie, Z., et al., J. Phys. Chem. C 112 (2008) 3935.
8. Quek, S. Y., Kamenetska, M., Steigerwald, M. L., Choi, H. J., Louie, S. G., Hybertsen, M. S., Neaton J. B., et al., Nat. Nanotechnol. 4 (2009) 230.
9. Klein, H., Blanc, W., Pierrisnard, R., Fauquet, C., & Dumas, P., Eur. Phys. J. B 14 (2000) 371.
10. Durig, U.; Novotny, L., Michel, B., Stalder, A., Rev. Sci. Instrum. 68 (1997) 3814.
11. Tsutsui, M., Shoji, K., Taniguchi, M., & Kawai, T., Nano Lett. 8 (2008) 345.
12. Candoni, N. et al., STM-BJ and MCBJ of gold nanowires: Statistics of the ballistic plateaus (To be submitted).
13. Suzuki, M., Niidome, Y., & Yamada, S., Thin Solid Films 496 (2006) 740.
14. Andreasen, G., Vela, M. E., Salvarezza, R. C., & Arvia, A. J., Langmuir 13 (1997) 6814.
15. Rubio, G., Agrait, N., & Vieira, S., Phys. Rev. Lett. 76 (1996) 2302.

16. Yanson, A. I., Bollinger, G. R., van den Brom, H. E., Agrait, N., & van Ruitenbeek, J. M., Nature 395 (1998) 783.
17. González, M. T., Wu, S., Huber, R., van der Molen, S. J., Schönenberger, C., & Calame, M., Nano Lett. 6 (2006) 2238.
18. Akkerman, H. B., Kronemeijer, A. J., van Hal, P. A., de Leeuw, D. M., Blom, P. W. M. & de Boer, B., Small, 4 (2008) 100. and Akkerman, H. B., Large-area Molecular Junctions, PhD thesis University of Groningen, The Netherlands (2008).